sciendo

Journal of MECHANICAL ENGINEERING – Strojnícky časopis,
VOL 68 (2018), NO 3, 261 - 270

STU SjF

THE INFLUENCE OF MATERIAL ON THE OPERATIONAL CHARACTERISTICS OF SPUR GEARS MANUFACTURED BY THE 3D PRINTING TECHNOLOGY

DIMIĆ Aleksandar[1], MIŠKOVIĆ Žarko[1], MITROVIĆ Radivoje[1], RISTIVOJEVIĆ Mileta[1], STAMENIĆ Zoran[1], DANKO Ján[2], BUCHA Jozef[2], MILESICH Tomáš[2]

[1] University of Belgrade, Faculty of Mechanical Engineering, Kraljice Marije 16, 11120 Belgrade 35, Serbia
[2] Slovak University of Technology in Bratislava, Faculty of Mechanical Engineering, Institute of Transport Technology and Designing, Nám. Slobody 17,812 31 Bratislava, Slovakia; jan.danko@stuba.sk

Abstract: The advanced development of additive technologies over the past years led to the fact that parts made by these technologies have been increasingly used in the most diverse engineering applications. One of the most famous and the most applied additive technology is 3D printing. In this paper the influence of the material type on the operational characteristics of spur gears manufactured by the 3D printing technology is analyzed, after the experimental testing performed on a back to back gear test rig, in the predefined laboratory conditions.

KEYWORDS: 3D printing technology, plastic spur gears, back to back gear test

1 Introduction

Spur gears are the most common elements for the transmission of power and motion from the group of mechanical power drives, Fig. 1.

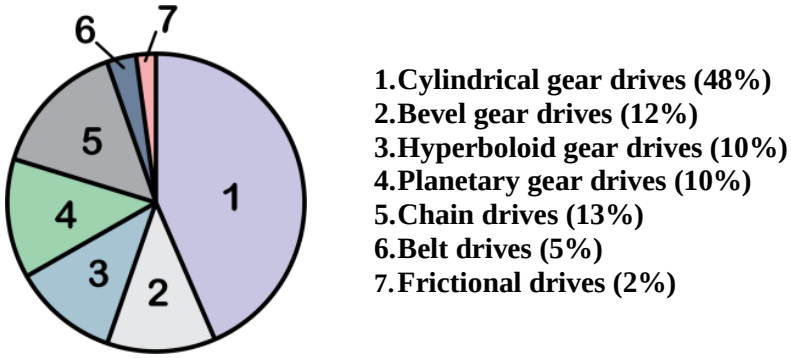

Fig. 1 Global spread of mechanical drives towards the end of 2005 [1]

Spur gears owe this role to the fact that they can achieve a relatively high transmission ratio and energy efficiency, they can be used for the transmission of high intensity power, they are also applicable at high speeds, and have a favourable mass to power ratio. For these reasons, even the smallest progress in the domain of calculation, material, construction and operational of spur gears is a significant contribution to mechanical engineering, and to engineering in general.

Spur gears are power transmission elements that are exposed to non-conforming operating conditions in terms of speed and load.

DOI: 10.2478/scjme-2018-0039, Print ISSN 0039-2472, On-line ISSN 2450-5471 ©2018 SjF STU Bratislava

Given their significant role in mechanical engineering, unlike some other mechanical elements whose load capacity is approximately determined on the basis of data on the testing of the mechanical characteristics of the samples, they are thoroughly examined at special-purpose test rigs. Probably the most famous test rig for testing spur gears is a back to back gear test rig (FZG[1] gear test), Fig. 2. A detailed description of this test rig can be found in [2]. Back to back gear test rig is a standardized laboratory test rig for testing spur gears with the purpose of obtaining data on the surface load capacity of the gear teeth flanks. The load is introduced into this system by the elastic torsion deformation of the shaft by the means of calibrated weights. After tightening the rigid coupling and removing weights, the electric motor only overcomes friction resistance of the system elements, including gears. Gear pairs are loading each other based on the principle of action and reaction, i.e. it creates an effect (illusion) that the power circulates in the closed circle. Thanks to its efficiency and applicability, a whole series of standardized procedures for testing the load capacity of gears teeth flanks to the various types of destruction [3-6] have been developed.

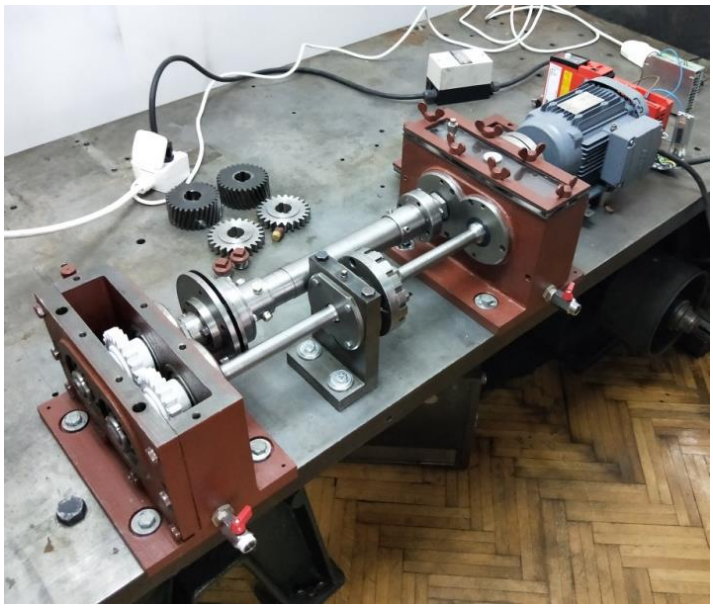

Fig. 2 Back to back gear test rig used in performed experimental research

All these procedures involve the testing of steel spur gears. However, for the scope of this paper, 3D printed spur gears made of plastics were tested on back to back gear test rig. These tests are directed towards increasing the use of parts produced by 3D printing, even in the most responsible structures (planes [7], spacecraft [8], etc.). Considering that in one of the previous papers [9] it was shown that by usage of 3D printing technologies spur gears with a satisfactory geometric accuracy can be made, so the question of their behaviour in real exploitation conditions is raised. For the purposes of this paper, two types of polymeric materials were analyzed. The initial load in the form of a torque that was exposed to the spur gears was held constant, while the number of revolutions per minute of spur gears was varied. The plastic gears tested in this experiment operated in unlubricated working conditions.

[1] FZG: Forschungsstelle für Zahnräder und Getriebebau - Technical Institute for the Study of Gears and Drive Mechanisms, Technical University Munich

2 Test samples

For a comparative analysis of the impact of the material on the operating performance of the spur gears manufactured by 3D printing, commercially available ABS (acrylonitrile butadiene styrene) and PLA (polylactide plastic) material were selected. A detailed description of the 3D printer used with the applied and explained printing parameters is shown in the paper [9]. Basic mechanical properties of the used materials are given in Table 1 [10]. The final shape of the additive manufactured spur gears is predefined by the 3D printing parameters. Some of the main parameters are explained below.

Table 1 Some properties of the used materials [10].

	Tensile strength [MPa]	Elongation[%]	Flexural Modulus [GPa]	Density [g/cm^3]	Melting point [°C]	Biodegradable	Glass transition temperature [°C]	Spool price (1kg, 1.75mm, black) [USD $]
ABS	27	3,5-50	2,1-7,6	1,0-1,4	N/A	No	105	21,99
PLA	37	6	4	1,3	173	Yes	60	22,99

Infill percentage

All material of the model that does not belong to the outer contours or partition shells is called infill. Infill provides the object with an internal support structure. The selected number of this parameter defines the solidity of the printed object. It can be concluded that more infill will increase the strength, but weight gain should be also significant. In addition to the weight limits, significant factors influencing the selection of infill percentage are printing time and 3D printer resources [11]. For the purposes of described experimental testing the infill percentage was selected to be 95%.

Printing angle

Based on previous experiences [12] and available scientific papers [13, 14] the printing angle is selected in order that the direction of the layers of the material coincides with the direction of the normal force which will act on the teeth flanks of the spur gear with involute profile. The formation of this printing angle is achieved by positioning the model on the printing platform in the manner shown in Fig. 3.

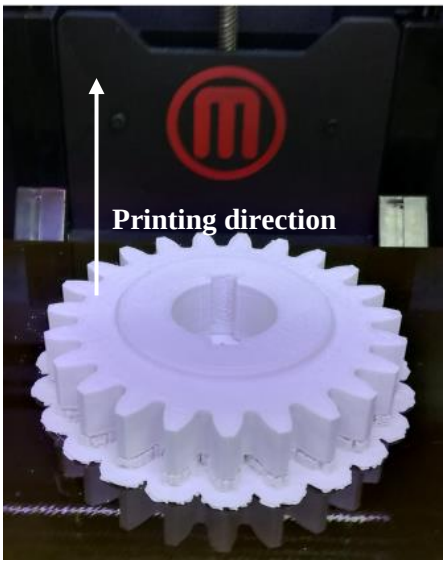

Fig. 3 Printing direction of the 3D printed spur gear

Layer height determines the thickness of each printed layer of the model. It is often treated as a measure of resolution in 3D printing, and consequently it is considered that the manufacturing accuracy largely depends on it, although it affects resolution only on the *z*-axis. Thinner layers will result in a smoother surface but will also increase print times; layers take the same time to print regardless of height but thinner layers increase the total number of layers to be printed. For the purposes of this experimental testing 0,3mm layer height was selected.Table 2 gives the parameters of the external gearing of spur gears designed to be fitted to the back to back gear test shown in Fig. 2. The spur gears parameters shown in Table 2 have been selected so that the tested gears are identical, which greatly facilitates the manufacturing and assembly process. An adverse consequence is that there are always the same teeth pairs in contact, which is the case that should be avoided in real working conditions.

Table 2 Parameters of tested spur gears

Dimension	Symbol		Numerical value	Unit
Shaft centre distance		a	91,5	mm
Effective face width		b	20	mm
Working pitch diameter	pinion wheel	d_{w1} d_{w2}	91,5	mm
Tip diameter	pinion wheel	d_{a1} d_{a2}	99,89	mm
Module		m	4	mm
Number of teeth	pinion wheel	z_1 z_2	23	
Profile shift coefficient	pinion wheel	x_1 x_2	-0,061	
Pressure angle		α	20	°
Working pressure angle		α_w	19,12	°
Overlap ratio		ε_α	1,69	

3 Experimental setup

The load capacity of spur gears is limited by surface and volume destruction. The most common types of bulk failures that are present in spur gears are static and dynamic teeth fractures. The most common types of surface degradation are wear, micropitting, pitting, scuffing. In standardized tests of metal gears in the back to back gear testing, the load regime, the rotational speed and gear geometry are defined depending on which type of destruction is examined. The above-mentioned surface destruction can be studied in a back to back gear rig testing. However, all these types of surface destruction are defined for the testing of metal spur gears and in the implementation of standardized procedures. In this experiment only plastic gears were examined. With metallic spur gears, the load in the form of torque increases at the appropriate levels while simultaneously controlling the process of surface destruction of the gear teeth flanks.

For the purposes of this experiment, the load in the form of a torque is fixed, that is, the initial moment of constant intensity has value 20 Nm. The torque of this intensity is insufficient to cause premature surface and volume destruction of spur gear teeth. The initially captured torque is "lost" during the wear process. The idea of this experiment was to estimate the wearing intensity for the initially captured load for two different spur gear materials.

The torque "loss" can be registered in several ways: using torque measuring clutch, by monitoring the temperature and vibration of the system, by monitoring the parameters of the

electric motor, and in this special case when plastic spur gears are examined with open housing - even visually.

The original concept of the back to back gear test involves a constant number of revolutions of the electric motor, however, in order to allow the variation of the rotational speed in this experiment, the frequency regulator is connected to the electric motor, with the possibility of varying the rotation number of electric motor from 0 to 1400 revolutions per minute (rpm). An increment of the rotational speed change of 200 rpm was adopted, with this speed being changed every 10 minutes during the test. This means that the maximum number of rotation of 1400 rpm is achieved after 60 minutes of testing.

The unlubricated operating conditions are selected so that monitoring of the spur gears meshing temperature field is enabled using thermal imaging methods. For this reason, during the gears testing, the casing of the tested gears was open, which further accelerated the cooling during the operation.

Operational behaviour of spur gears can be traced in several different ways. Some of the indicators most commonly used for operational analysis of spur gears are: noise and vibration levels [15], temperatures [16, 17], quantity and shape of wear products [18], etc. In order to perform the analysis of the influence of material on the operational characteristics of spur gears manufactured by the 3D printing technologies, temperature and vibration were selected as the main indicators. In the last few years, due to the ease of use and the provision of reliable data, the use of thermo-optical methods for the monitoring of temperature changes in the analysis of the operational behaviour of mechanical systems is becoming more frequent. [19-21] One of the main advantages of this method, in relation to some of the classic methods (for example, the use of thermocouples), is that it gives high accuracy data about the whole temperature field and not just about one particular selected point of the system.

The meshing temperature field of plastic spur gears in this work was recorded using advanced thermal imaging camera: Thermal camera IRC57 InfraCAM SD, manufactured by FLIR Co. (USA), with temperature measurement range of 10-350°C, and ±2% accuracy [22]. Taking into account that plastic gears are tested as well as the sensitivity of plastic to the presence of increased temperatures it is necessary to determine the highest temperature in the meshing temperature field as precise as possible.

The direction of rotation of the electric motor as well as test gears, Fig. 4, is so adjusted that the position of the recording allows "capturing" the temperature field of the spur gear teeth immediately after their exit from the contact (meshing). After the image “capturing”, the software is used for the indication of the highest registered temperature in the temperature field, Fig. 5, which in this case were the active surfaces of the spur gear teeth flanks after carrying out the load transfer. In order to obtain as reliable data as possible, it is necessary to know the emissivity coefficient of the material from which the machine part, whose surface is being recorded, is made of.

The emissivity coefficient of the white plastic from which the spur gears were manufactured using 3D printing technology is $\varepsilon = 0{,}84$ [23] (Emissivity Coefficient for white plastic: 0,84). Temperature field image was “captured” after every minute of the testing, until the end of experiment. Then obtained results were then analyzed in the corresponding software.

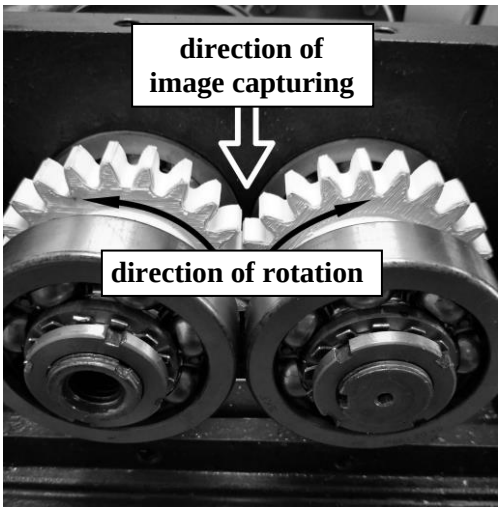

Fig. 4 Direction of rotation and direction of image capturing

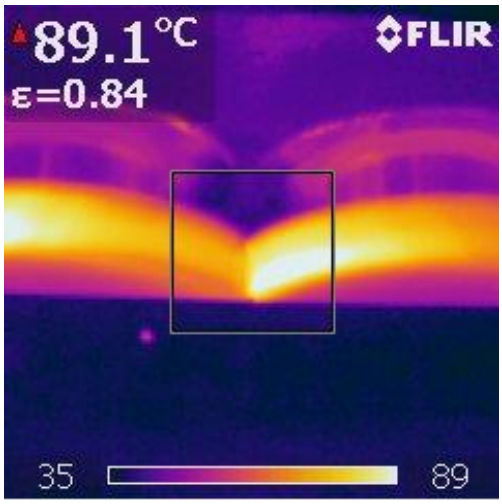

Fig. 5 Highest measured temperature on the contact surfaces of tested gears

As far as vibrodiagnostics is concerned, it has long occupied the site as one of the most reliable parameters for evaluating the operational behaviour of machine structures. SKF Microlog Analyzer GX was used to collect information on the vibrations (RMS acceleration) of the tested gears [24, 26]. A single-axis sensor CMSS 2111 [25, 27] was used, which registered the data on the vibration level of the housing of the tested gears in the radial direction and which was positioned in the place indicated in the Fig. 6. Knowing the number of teeth of the tested spur gears, as well as their number of revolutions, a change in the amplitude of the vibration level is observed over time, by distinguishing the peak resulting from the meshing of the plastic spur gears.

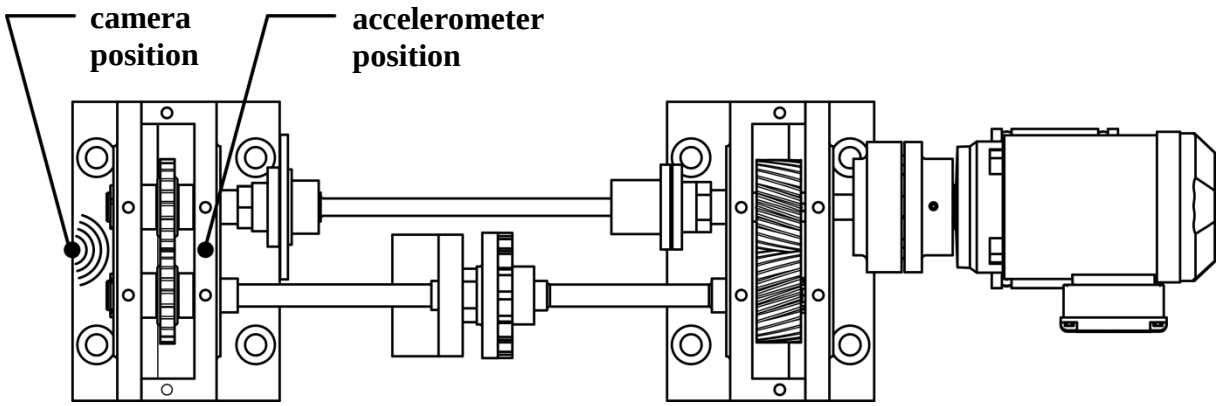

Fig. 6 Schematic view of back to back gear test rig with measuring positions

4 Analysis of the results

The two parameters were observed during the experiment, temperature and vibration (RMS acceleration) change in time with rotational speed increasing, on spur gears manufactured from different kinds of plastics (ABS and PLA). The results are shown on Fig. 7 and Fig. 8. On both diagrams it can be seen that gears manufactured from ABS plastic endured about 30 minutes of work, and at 600 rpm their teeth have been experienced failure in the form of teeth breakage.

All of the broken teeth were fractured in tooth root area, Fig. 9. The gears manufactured from PLA plastic endured much longer (90 minutes at max. 1400 rpm), without any visible fracture, but with evident teeth contact surface destruction, Fig. 10.

The graph, Fig. 7, of temperature change in time with increment of rotation speed (rpm) shows that in first 10 minutes of experiment under 200 rpm, the temperature of PLA plastic gear pairs is higher than those made of ABS plastic (difference equals roughly 20%). With an increase of the rotational speed from 400 to 600 rpm, the highest temperature of PLA plastic gears contact surface is almost stabilized (oscillates around ~80°C), while highest temperatures of ABS gears drastically increases (up to 125°C).

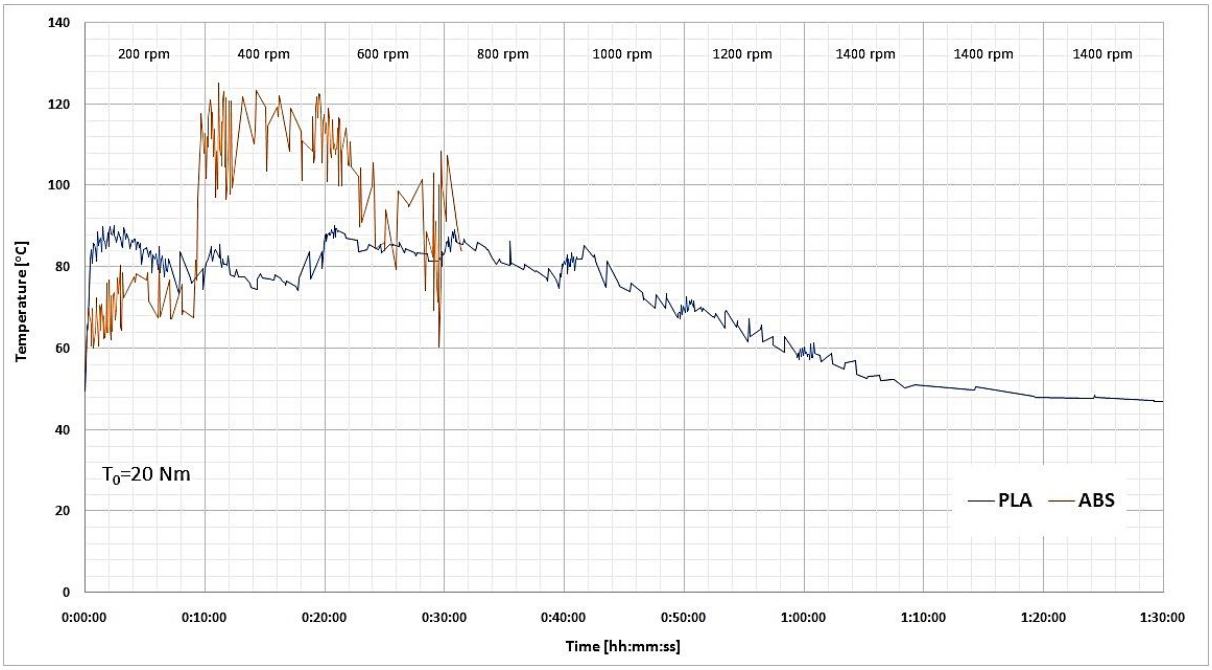

Fig. 7 Contact temperature change of the gear teeth flanks during the experiment

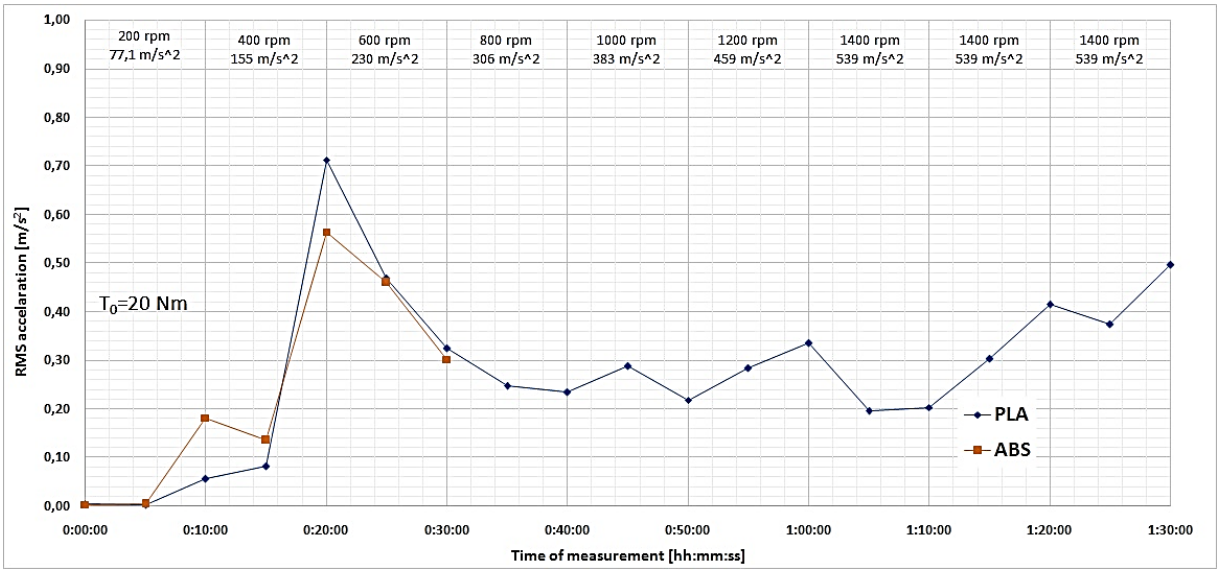

Fig. 8 Meshing vibration (RMS Acceleration) change during the experiment

A vibration (RMS acceleration) in time dependence from rotational speed is shown on Fig. 8. It can be noticed that in the first 5 minutes of experiment under 200 rpm, there is almost no vibration.

In the interval from 5 to 15 minutes, vibrations behaviour of ABS and PLA plastic gear pairs is inverse comparing to their thermal behaviour (temperature change in time, Fig. 7). The vibrations of ABS plastic gears is higher (RMS=0,18 ms^{-2}) than the ones made of PLA plastic (RMS=0,06 ms^{-2}). Increasing the rotational speed from 300 up the 400 rpm, the vibration of both gear pairs significantly rises (up to RMS=0,72 ms^{-2}). After 400 to 500 and 600 rpm, the vibration levels are declining. After 30 minutes of testing with 600 rpm, just before tooth of ABS gear pair fractured, the level of RMS accelerations was 0,3 ms^{-2}. The vibration level of PLA plastic gear pair vary with an increase of rpm and oscillate around 0,25 ms^{-2}. At the end of experiment (on 1400 rpm) the vibration values of PLA plastic gear pair is increasing to 0,5 ms^{-2}, probably due to gear tooth contact surface destruction.

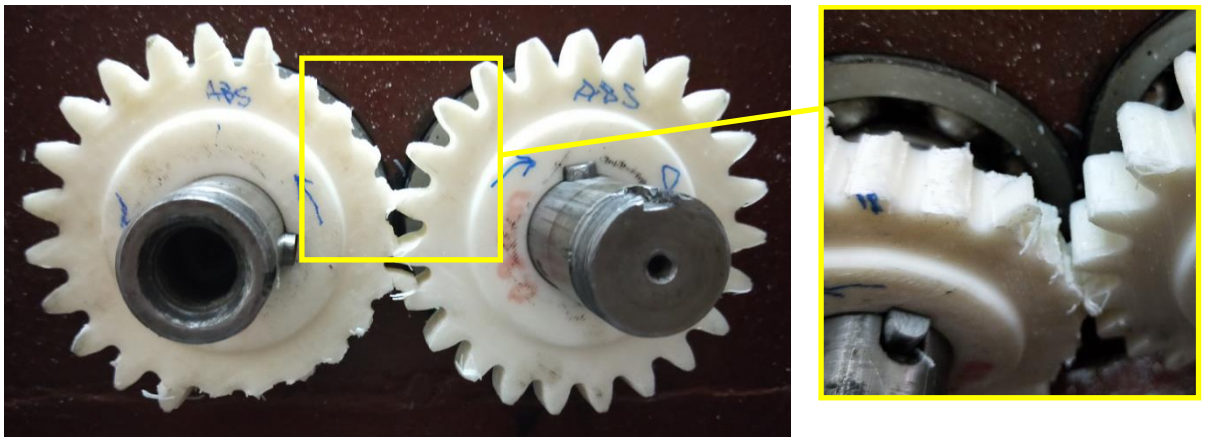

Fig. 9 Failure at the teeth roots of the tested ABS gears

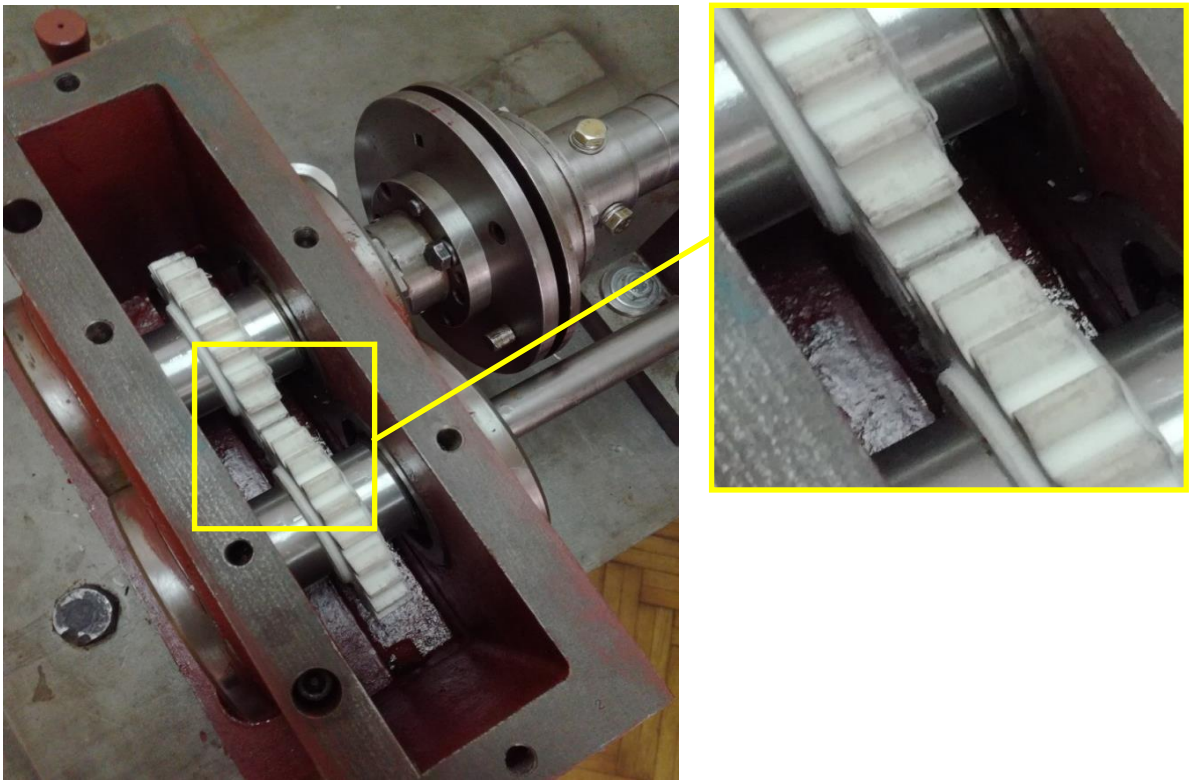

Fig. 10 Worn off teeth flank surfaces of the tested PLA gears

CONCLUSION

From the performed experiments, it can be concluded that the 3D printed spur gears manufactured from PLA plastic have better operational characteristics than the ones manufacture from ABS plastic. Bearing in mind that this is the beginning of the more comprehensive research, only two gear pairs manufactured of ABS and PLA plastics were examined. It is obvious that, by repeating the experiment with more samples (more gear pairs), using the same testing parameters, the more statistically accurate data will be obtained, which is planned to be done in the continuation of the research. In the future experimental research it's also planned to vary the 3D printed gears test samples layer thickness, as well as the infill percentage of manufactured prototypes.

ACKNOWLEDGEMENT

The authors would like to express their gratitude to the Slovak Research and Development Agency and to the Ministry of Education, Science and Technological Development of Republic of Serbia for the support of the bilateral project No. SK-SRB 2016-0054, as well as for the equipment used, which was acquired within the project TR35029.

REFERENCES

[1] D. Jelaska. Gears and gear drives, John Wiley & Sons Ltd, **2012**, ISBN 978-1-119-94130-9.

[2] K. Michaelis, H. Winter. Development of a high temperature FZG-ryder gear lubricant load capacity machine (Wright Research and Development Center, **1989**). Identification number F49620-86-C-0081.

[3] ISO 14635-1:2000 Gears -- FZG test procedures -- Part 1: FZG test method A/8,3/90 for relative scuffing load-carrying capacity of oils.

[4] ISO 14635-2:2004 Gears -- FZG test procedures -- Part 2: FZG step load test A10/16, 6R/120 for relative scuffing load-carrying capacity of high EP oils.

[5] ISO 14635-3:2005 Gears -- FZG test procedures -- Part 3: FZG test method A/2, 8/50 for relative scuffing load-carrying capacity and wear characteristics of semifluid gear greases.

[6] B.R. Höhn, G. Steinberger. Test methods for Lubricant Related Influences on the Gear Load Capacity (Lubricants Russia **2006**, 2nd international conference).

[7] T. Kellner. GE Reports website (2016), Fit to print: New Plant Will Assemble World's First Passenger Jet Engine with 3D printed Fuel Nozzles, Next-Gen Materials, http://www.gereports.com/ (accessed on 1 June **2016**).

[8] H. Krueger. Standardization for Additive Manufacturing in Aerospace. *Engineering* **2017** (3), No. 5: 585. DOI: 10.1016/J.ENG.2017.05.010

[9] R. Mitrović, Ž. Mišković, M. Ristivojević, A. Dimić, J. Danko, J. Bucha, M. Rackov. Determination of optimal parameters for rapid prototyping of the involute gears. *IOP Conference Series: Materials Science and Engineering* **2018** (393). DOI: 10.1088/1757-899X/393/1/012105

[10] 3Dhubs. PLA vs. ABS: What's the difference? https://www.3dhubs.com/ (accessed on March **2018**.)

[11] MakerBot. Replicator 2X–Experimental 3D printer. User Manual. https:// http://downloads.makerbot.com (accessed on March **2018**.)

[12] R. Mitrović, Ž. Mišković, M. Ristivojević, A. Dimić, J. Danko, J. Bucha, M. Rackov. Statistical correlation between the printing angle and stress and strain of 3D printed models under static axial loading. ECF22 - Loading and Environmental effects on Structural Integrity, **2018**.

[13] T. Letcher, B. Rankouhi, S. Javadpour. Experimental study of mechanical properties of additively manufactured abs plastic as a function of layer parameters. *Proceedings of the ASME 2015 International Mechanical Engineering Congress and Exposition*, Houston, Texas, Nov.13 – 19, **2015**, 1–8.

[14] A. R. T. Perez, D. A. Roberson, R. B. Wicker. Fracture Surface Analysis of 3D-Printed Tensile Specimens of Novel ABS-Based Materials. *J Fail. Anal. and Preven.* **2014** (14), 343 – 353.

[15] M. Åkerblom. Gear noise and vibration – a literature survey (Volvo Construction Equipment Components AB SE–631 85 Eskilstuna, Sweden).

[16] K. Terashima, N. Tukamoto, N. Nishida. Development of plastic gears for power transmission - Design on load carying capacity. *Bulletin of JSME* **1986** (29), No. 250, 1326 – 1329.

[17] C. J. Hooke, K. Mao, D. Walton, A. R. Breeds and S. N. Kukureka. Measurement and Prediction of the Surface Temperature in Polymer Gears and Its Relationship to Gear Wear *J. Tribol* **1993** (115), No. 1, 119 – 124.

[18] L. Jia-Jun, C. Yu, C. Yin-Qian. The generation of wear debris of different morphology in the running-in process of iron and steels. *Wear* **1992** (254), 259 – 267.

[19] Ž. Mišković, R. Mitrović, Z. Stamenić. Analysis of grease contamination influence on the internal radial clearance of ball bearings by thermographic inspection. *Thermal Science* **2016** (20), No. 1, 255 – 265.

[20] A. Glowacz, Z. Glowacz. Diagnosis of the three-phase induction motor using thermal imaging *Infrared Physics & Technology* **2017** (81), 7 – 16.

[21] M. Fidali. An idea of continuous thermographic monitoring of machinery (9th International Conference on Quantitative InfraRed Thermography, **2008**).

[22] Extech IRC57 InfraCam SD Thermal Imaging Camera, http://www.instrumentation2000.com/.

[23] Thermowork Inc. Emissivity Table (https://www.thermoworks.com/emissivity_table).

[24] SKF USA Inc. Condition Monitoring Center. The SKF Microlog series catalogue. SKF Group, Livingston, **2018**.

[25] SKF USA Inc. Condition Monitoring Center. SKF Microlog Analyzer Accessories Catalog. SKF Group, San Diego, **2018**.

[26] R. Jančo, L. Écsi, P. Élesztős. FSW Numerical Simulation of Aluminium Plates by SYSWELD - Part II. *Strojnícky časopis – Journal of Mechanical Engineering* **2016** (66), No. 2, 29 – 36. DOI: 10.1515/scjme-2016-0016

[27] P. Élesztős, R. Jančo, V. Voštiar. Optimization of Welding Process using a Genetic Algorithm. *Strojnícky časopis – Journal of Mechanical Engineering* **2018** (68), No. 2, 17 – 24. DOI: 10.2478/scjme-2018-0014